A generalized iterative back-projection algorithm for 2-D reconstruction of resistivity data: application to data-sets from archaeological sites

P. TSOURLOS[1], J. E. SZYMANSKI[2] and G. N. TSOKAS[1]

[1]*Department of Geophysics, Aristotle University of Thessaloniki, 54006 Thessaloniki, Greece.*

[2]*Dept. of Electronics, University of York, Heslington, York Y01 5DD, U.K.*

Abstract: In this work a generalized iterative back-projection algorithm for the 2-D reconstruction of resistivity data is proposed. The need for such an algorithm derives from the analysis of the limitations of the existing approximate algorithms. Further, it can reconstruct data from any array as well as from unconventional electrode arrangements. The merits and limitations of the algorithm are discussed and examples of its performance with synthetic data are given. Extensive tests of the algorithm with real data obtained from archaeological sites are presented as well. Despite its inherent limitations the algorithm proved to be reliable and noise insensitive and produced good quality reconstructions.

Key Words: 2-D Resistivity Reconstruction, Back-projection, Archaeological Prospecting.

INTRODUCTION

Electrical resistivity techniques are well-established and applicable to a wide range of geophysical problems (Telford et al., 1989). In archaeological prospection, resistivity mapping has been in use for many years but tend to be used in a qualitative fashion for simple detection. 2-D resistivity measurements can give information about both the lateral and vertical variations of the subsurface resistivity and can be used in a qualitative fashion for the identification of the structure and depth of archaeological features.

The potential use of 2-D resistivity prospection is of increasing interest due to the development of automatically multiplexed measuring systems which facilitate the acquisition of a large number of measurements in a limited time (Griffiths et al., 1990; Noel and Walker 1991; Dahlin, 1992). This development gives the resistivity method an increased operational flexibility. However, it is essential to develop reliable and robust interpretation-inversion algorithms which are able to produce a "deblurred" resistivity image in order to render the information accessible to non-experts (i.e. field archaeologists).

The traditional methods of data interpretation, such as the construction of a pseudosection (Edwards, 1978) provide only a rather qualitative insight into the region of interest and moreover they can only cope with the traditional (surface linear-arrays, set range of spacings) measuring schemes. Another interpretation method is an operator-controlled data fitting technique which involves the repetitive use of a forward resistivity modelling scheme (eg. Stretenovic and Marcetic, 1992). Due to its non-automatic nature this method is impractical for handling large data-sets.

The resistivity inverse problem involves constructing an estimate of a subsurface resistivity distribution which is consistent with the experimental data. This is a fully non-linear problem and its treatment involves iterative full-matrix inversion algorithms which can give good quality results (Trip et al., 1984; Smith and Vozoff, 1984) but these algorithms can be quite costly in terms of computer time and memory. More recent developments involve acceleration of the inversion procedure by the use of quasi-Newton techniques for updating the Jacobian matrix in every iteration. An alternative strategy towards resistivity inversion is to use approximate

schemes, which, despite their intrinsic theoretical weaknesses, can produce reasonably valid sectional images of the subsurface resistivity pattern in a fairly short time. The need for such fast algorithms is increased by the development of automatic measuring systems which can result in a huge increase into the amount of recorded measurements.

Approximate algorithms handle the inversion problem as a linear one and they serve as a tool for preliminary interpretation of the experimental data-sets. For most approximate resistivity reconstruction techniques it is only physical intuition rather than a solid mathematical background which is used to justify why they do work and, furthermore, it is quite possible to produce results which can lead to erroneous interpretations. A detailed study of the properties and limitations of several approximate resistivity reconstruction techniques can be found in Tsourlos (1995).

In this work we will investigate a particular class of linearized reconstruction methods which are based on the use of the back-projection (BP) technique. Related algorithms have been developed for the medical imaging research field, and in particular for a technique called applied potential tomography (APT) (Barber et al., 1983; Yorkey et al. 1987). Broadly speaking, the BP technique (for the earth-resistivity case) involves the direct projection of an expression of the measured apparent resistivity measurements into an area of the subsurface. Projection of the entire data-set results into an "approximate" image of the subsurface. In that sense techniques such as the pseudosection, the related Zhody-Barker technique (Barker, 1992) and the Bristow method (Bristow, 1966) can be viewed as simple BP techniques.

A BP method was first used for earth resistivity data-sets by Shima and Sakayama (1987) who proposed a one-step back-projection reconstruction algorithm using the entries of the sensitivity matrix as the weighting factors for the BP. In a later work Shima (1992) used this algorithm in order to obtain an initial guess for a fully non-linear inversion. Noel and Walker

(1991) proposed a BP algorithm which was based on work done for APT (Powell et al, 1987): their one step BP procedure was constrained to areas defined by pairs of equipotential lines. The BP was weighted by the use of the sensitivity matrix entries corresponding to these points.

Here, the BP method is extended to an iterative self-correcting-approach. Although the scheme can be used for the reconstruction of borehole-to-borehole or borehole-to-surface data-sets, we will restrict this work to surface-to-surface measurements and in particular to the well known resistivity arrays. The initial intention is to illustrate the improvements possible even with only a restricted 'traditional' data set.

The iterative algorithm is based on the repetitive use of a realistic forward modelling scheme: the finite element method (FEM) was chosen since it has already been widely used in resistivity modelling and has the advantage that it can cope with irregular shapes and boundaries, therefore can incorporate possible terrain anomalies which could be a significant source of noise within the measurements.

During the reconstruction procedure the resistivity distribution in terms of the model space is expressed as a set of homogeneous blocks (parameters) which are allowed to vary their resistivity independently. In the proposed scheme, it is necessary to use a matrix, the Jacobian J, which associates variations in the property of those parameters with variations in the observed data. The calculation of the Jacobian matrix was made within the framework of the FEM technique.

The technique presented in this work was tested using a series of synthetic data-sets. Four of the models which were used to produce the synthetic data are depicted in Figure 1. We will be referring to those models as Model 1 (one resistive prism), Model 2 (vertical discontinuity), Model 3 (two resistive prisms), Model 4 (conductive layers and a resistive prism).
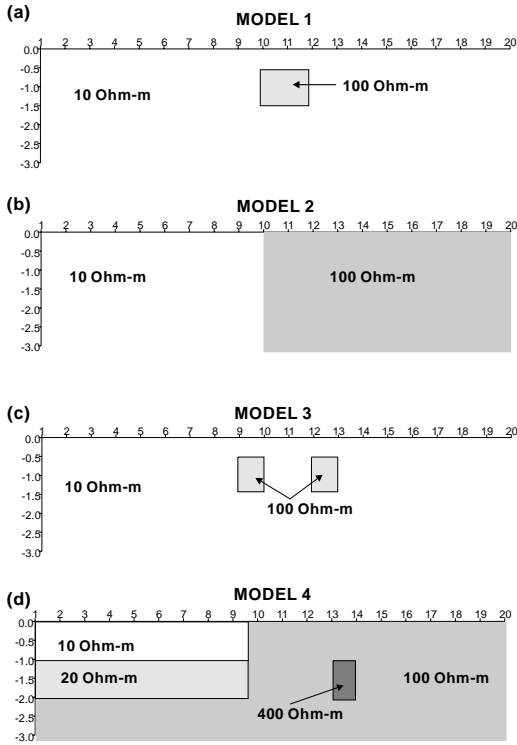
FIG. 1: The synthetic models used in this work: a) Model 1 (one resistive prism), b) Model 2 (vertical discontinuity), c) Model 3 (two resistive prisms), d) Model 3 (conductive layers and resistive prism).

THE FORWARD MODELLING SCHEME USED

The forward model calculations presented in this work were made using the finite element method (FEM). The technique has been extensively described in many works (Coggon 1971; Rijo 1978) so only a brief description of the method is presented here. A 2.5-D model was used: the source is considered to be 3-D but the subsurface resistivity is only 2-D. To include the potential variability at the strike (y) direction a cosine Fourier transformation is applied. The FEM solves the governing (Helmholtz's) equation by discretizing the earth into homogeneous triangular (in our case) regions called elements. The potential within each element is approximated by a simple interpolation function which is called basis function and which is related to the potential at the vertices (nodes) of each triangle. In order to minimize the error between the approximated and real potential, the Galerkin minimization criterion is applied (the basis function should be orthogonal to the potential). After applying the Galerkin minimization scheme

to every element, and since triangular elements will share common nodes, the individual element equations can be assembled into one global system that has the following form:

$$\mathbf{K} \cdot \mathbf{A} = \mathbf{F} \tag{1}$$

where A is the unknown transformed nodal potential vector, F is the a vector describing the sources and K is a matrix which is related to the nodal coordinates. After applying the homogeneous Dirichlet and Newman boundary conditions the system of eq. (l) is being solved and the transformed nodal potential is obtained. After solving eq. (1) for several wavenumbers, the total potential is recovered by applying the inverse Fourier transform. Since the nodal potential is known point-to-point potential differences and apparent resistivities are easily obtained.

A GENERALIZED ITERATIVE BACK-PROJECTION ALGORITHM

In this section, a generalized back-projection algorithm for reconstructing earth-resistivity data is presented. The need for such an algorithm derives from an analysis of the limitations of the existing approximate algorithms.

The presented algorithm can be classified as general for several reasons:

a. It can include all of the presented BP algorithms (the methods of Bristow, Powell, Noel, and Shima) as well as techniques such as the pseudosection and Barker's method.

b. It can be iterative and in this way it can produce a quantitative "image" of the subsurface resistivity.

c. It can reconstruct data from any array as well as from unconventional probe arrangements and full tomographic data. Further, it can reconstruct incomplete data.

The proposed iterative technique seeks to obtain an estimate of the subsurface resistivity distribution for which the predicted measurement values (obtained by the solution of the forward problem) are as close as possible to the measured data. In order to achieve this, an initial resistivity distribution is assumed (usually uniform) and by using the forward modelling technique, the

modelled measurements that correspond to this distribution are obtained. These modelled measurements are compared with the original data and the weighted differences are back-projected in order to obtain a correction to the resistivity estimate. This correction is added to the current resistivity distribution and the procedure is repeated until the difference between the measured and the modelled data satisfies a stopping criterion.

Let the M measured data values obtained by using a tomographic measuring scheme be represented by a vector D where $D^T=\{D_1,D_2,...D_M\}$, and let d be the vector which represents the modelled data, $d^T=\{d_1,d_2,...d_M\}$. The N subsurface blocks that are allowed to vary their resistivity independently (the unknown parameters of the problem) are represented by a vector x with $x^T=\{x_1,x_2,...x_N\}$. The iterative procedure can be defined as:

- x^k is the resistivity estimate at the kth iteration;

- Calculate the modelled data set d^k that corresponds to this resistivity distribution by using the FEM;

- Find the new resistivity correction vector dx^k. The resistivity correction estimate at every block j will be:

$$dx_j^k = \frac{\sum_{i=1}^{M}(D_i - d_i^k)W_{ij}^k}{\sum_{i=1}^{M}W_{ij}^k} \ ,$$

where W_{ij} is the weighting factor which for our case is Jacobian matrix entry for the k iteration which corresponds to block j and measurement i;

- The new resistivity estimate x^{k+1} will be : $x^{k+1}= x^k+dx^k$;

- Repeat until the RMS between the measured and modelled data is practically stable (i.e. less than 3% improvement), or if divergence occurs, or if a preset number of iterations has been reached.

This procedure has similarities to the simultaneous iterative reconstruction technique (SIRT) in the sense that the resistivity corrections are taking place after the entire data-set has been

back-projected. Eq. (2) describes the back-projection procedure. The resistivity correction for each block is the sum of the weighted differences between the observed and the modelled data.

The weighting factor can play a significant role in the BP procedure since each subsurface parameter contributes to each individual surface measurement to a different extent. By using parts of the JM as a weighting factor this varying sensitivity of the parameters towards the measurements is reflect into the reconstruction. Since in every iteration the resistivity distribution changes are followed by the Jacobian matrix changes as well. Therefore, the Jacobian matrix is updated in every iteration.

CONSTRAINING BACK-PROJECTION

For linear resistivity arrays usage of the entire JM within the BP procedure resulted into negative subsurface resistivitiess. Although the reconstructed image was quite close to the original structure, invalid negative resistivities were produced at the parameters which are located at the top of the reconstructed area - this did not change when the size of these parameters was increased.

This irregularity can be explained by the very large values of the Jacobian matrix which are associated with these parameters. Because of the approximate nature of the technique, these large Jacobian values will exaggerate the resistivity correction for the top layer parameters and will produce ``unreasonable'' results. Note that this problem was also mentioned by Shima (1992) who observed similar results when he tried to reconstruct crossborehole-to-surface data sets.

In order to tackle this problem, it is common to apply some constraints in order to use only parts of the Jacobian matrix. Instead of using arbitrary constraints such as that of the equipotential lines we suggest the use of a constraint which is directly related to values of the Jacobian matrix. Taking into account the direct link between the JM and the BP procedure such a constraint allows the application of the BP in any type of resistivity data.

If a threshold value t is defined the weighting factor W_{ij} of eq. (2) is given by:

$$W_{ij} = \begin{cases} J_{ij} & \text{if } J_{ij} \geq t \\ 0 & \text{otherwise} \ . \end{cases}$$

This threshold value can be decided after several tests. In particular, model tests were carried out in order to find the optimum value which is the highest possible one that does not affect the produced image. For most arrays the value $t=0$ (which excludes all the negative sensitivity entries) was a valid choice.

In Figure 2a comparison between this constraint and the equipotential line constraint (Noel, 1992) for the dipole-dipole data can be seen. It is clear that this proposed threshold allow a larger part of the sensitivity matrix to participate in the reconstruction and that the equipotential constraint is a high threshold.
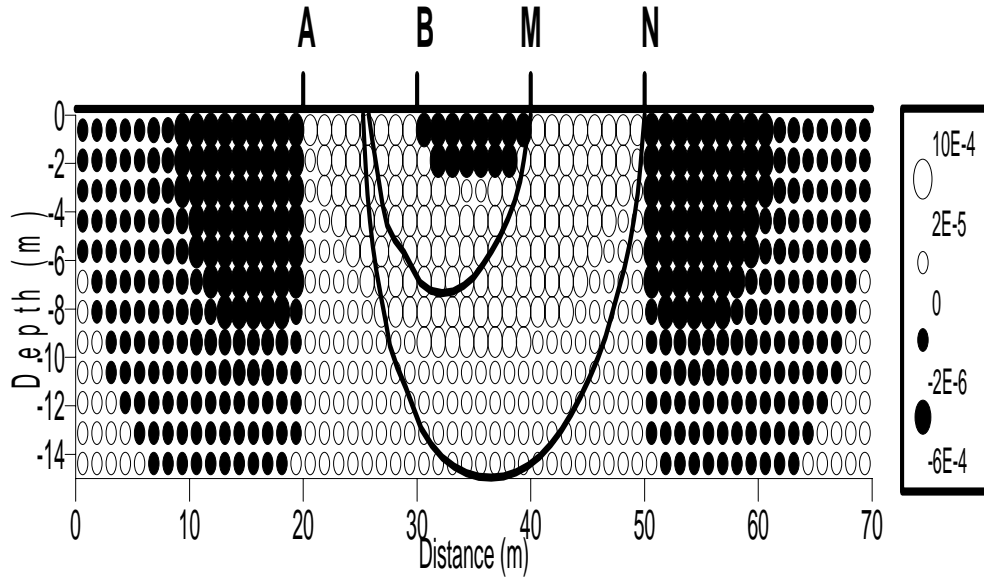

**FIG. 2:** A comparison between the equipotential line and the generalized constraint.

RECONSTRUCTION EXAMPLES

A computer program was written in order to enable the automatic reconstruction of surface resistivity data. The FEM was used as to calculate the forward model response and the Jacobian matrix. The size of each parameter region was set to be a square with a side of half inter-electrode spacing. The number of parameters in each layer is symmetrically reduced as depth increases since the parameters at the edges are not well-resolved. Outside the parametrized area the element resistivities were set to be equal to that of the nearest side or bottom parameter. Several tests

were conducted to validate the algorithm. The dipole-dipole data-set for Model 1 was reconstructed using one iteration of the generalized algorithm. The results are shown in Figure 3a. In Figure 3b the results for the same model after 10 iterations are shown. The quantitative results are not that close to the original ones. Despite this fact there is no doubt that the iterative procedure delineates the target far better than the non-iterative scheme. The convergence behaviour for this reconstruction can be seen in Figure 4: during the first few iterations the RMS error reduces rapidly while in the following iterations the convergence rate becomes almost linear.
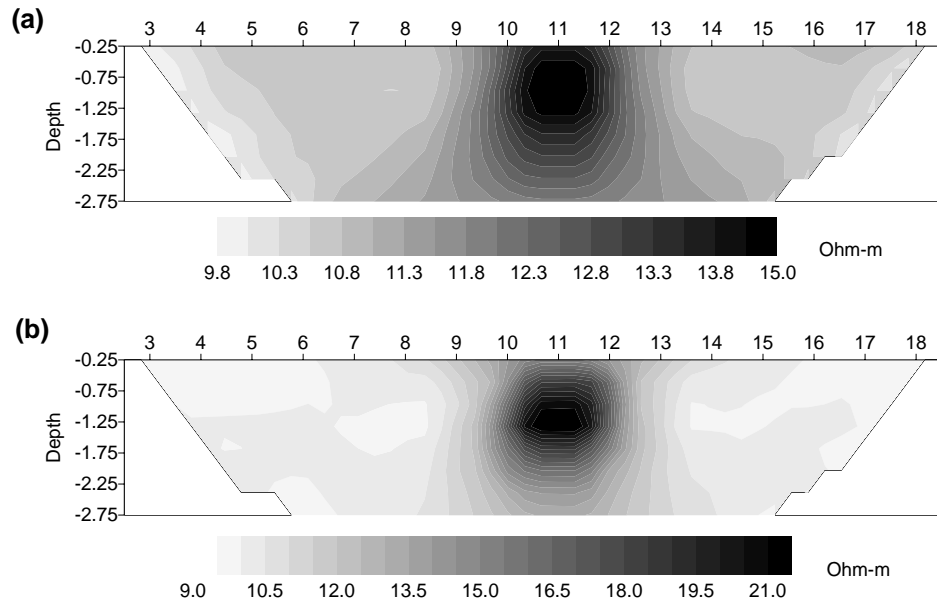
FIG. 3: Reconstruction of Model 1 (dipole-dipole data): a) generalized BP (1 iteration), b) generalized BP (10 iterations).
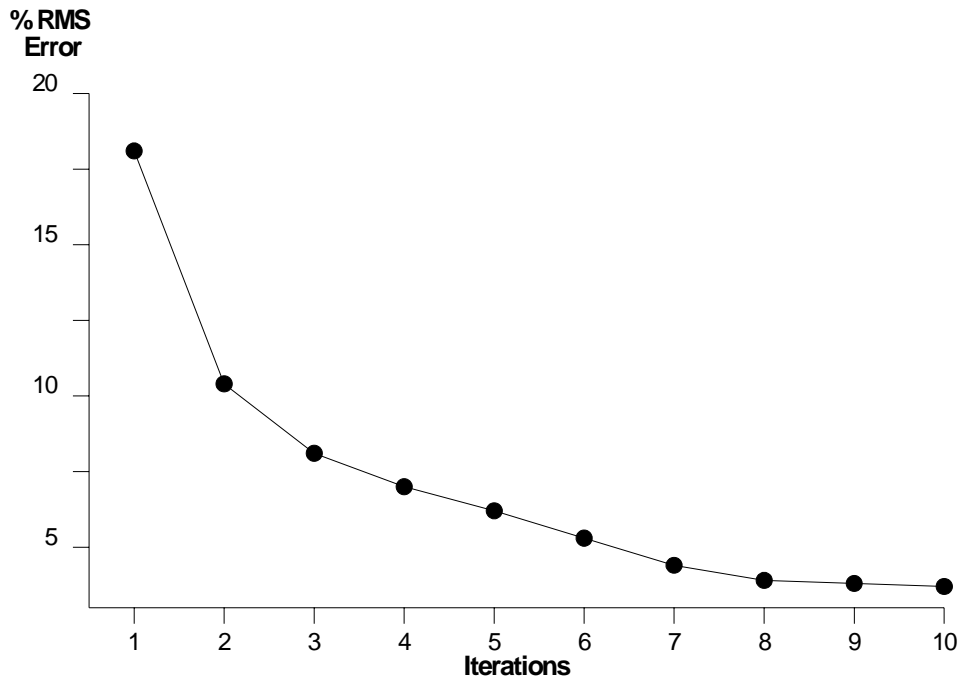
FIG. 4: The RMS error curve for the reconstruction of the dipole-dipole set for Model 1.

This convergence pattern was similar for all the tested cases. The calculation of the Jacobian at every iteration is important in speeding up the convergence but on the other hand, calculating the Jacobian at every iteration is time consuming and therefore the Jacobian is updated only during the first iterations where the RMS drops fast (indicating in this way sizable changes in the resistivity distribution) and afterwards only every other 3 iterations. This reduces the time that the reconstruction takes without significantly affecting the convergence. A simplified flow-chart of the algorithm is shown in Figure 5.
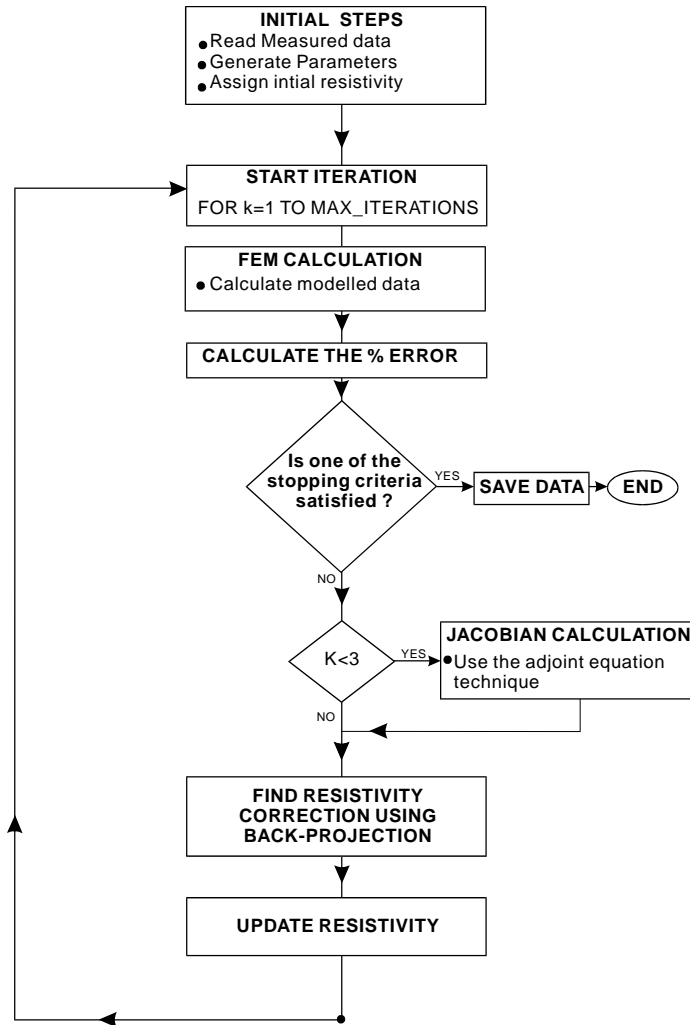
**FIG. 5:** A simplified flow-chart of the algorithm.

In Figure 6 the reconstruction results using several known arrays are shown. The reconstruction of the Wenner and pole-dipole data-sets for Model 1 is depicted in Figures 6a, 6b. In Figure 6c the reconstruction of Model 2 for pole-pole data is shown. The results indicate that the technique can be used for reconstructing data-sets obtained from any array. For all reconstructions only the positive entries of the Jacobian matrix were considered. Note that for the pole-dipole array the full data-set was considered (both A, M-N and N-M, A arrangements) since using only the data-set for the arrangement (A, M-N) results into an asymmetric reconstruction. Several other tests were conducted with a variety of synthetic models. In Figure 7 the reconstructions for the dipole-dipole modelled data from Models 2, 3, 4 are shown. In all of the examples the maximum dipole separation was six dipole lengths (n=6) and the entire measuring pattern included 20 measuring probes. The data-sets were corrupted with 5% Gaussian noise. The results indicate that the algorithm can give reliable reconstructions which delineate the subsurface structures fairly well in a qualitative fashion and give a reasonable quantitative approximation. Further, the algorithm behaved well with noisy data and it still retained its stability. No major artefacts appeared which could indicate an inherent problem of the algorithm towards noisy data. Stability problems appeared only when the level of the noise was very high.
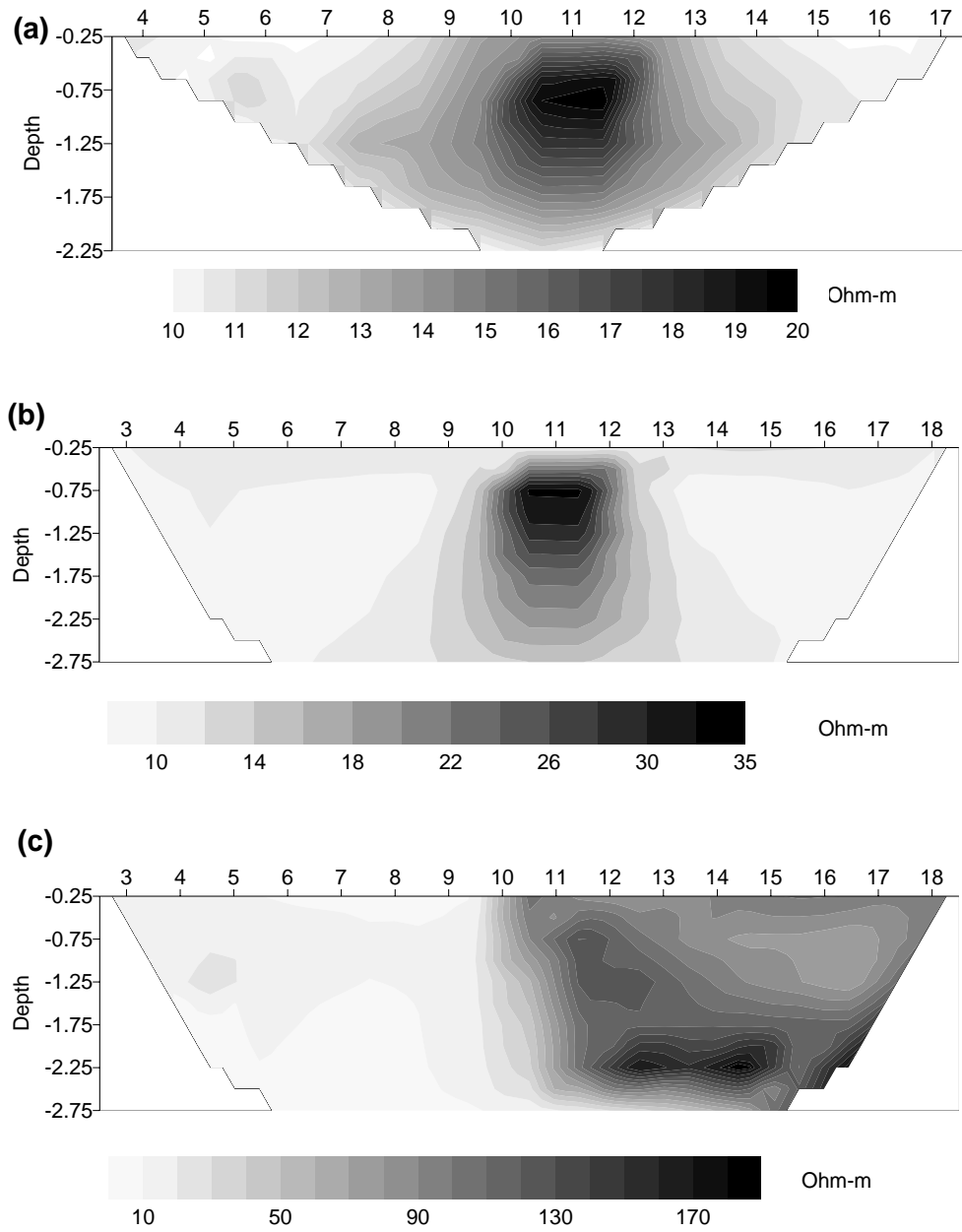
FIG. 6: Reconstruction of Model 1 using the generalized BP scheme: a) Wenner data-set (10 iterations, 2.8% RMS error), b) pole-dipole data-set (11 iterations, 3.5% RMS error). c) Reconstruction of Model 2 using the generalized BP scheme for pole-pole data (8 iterations, 4.2% RMS error).
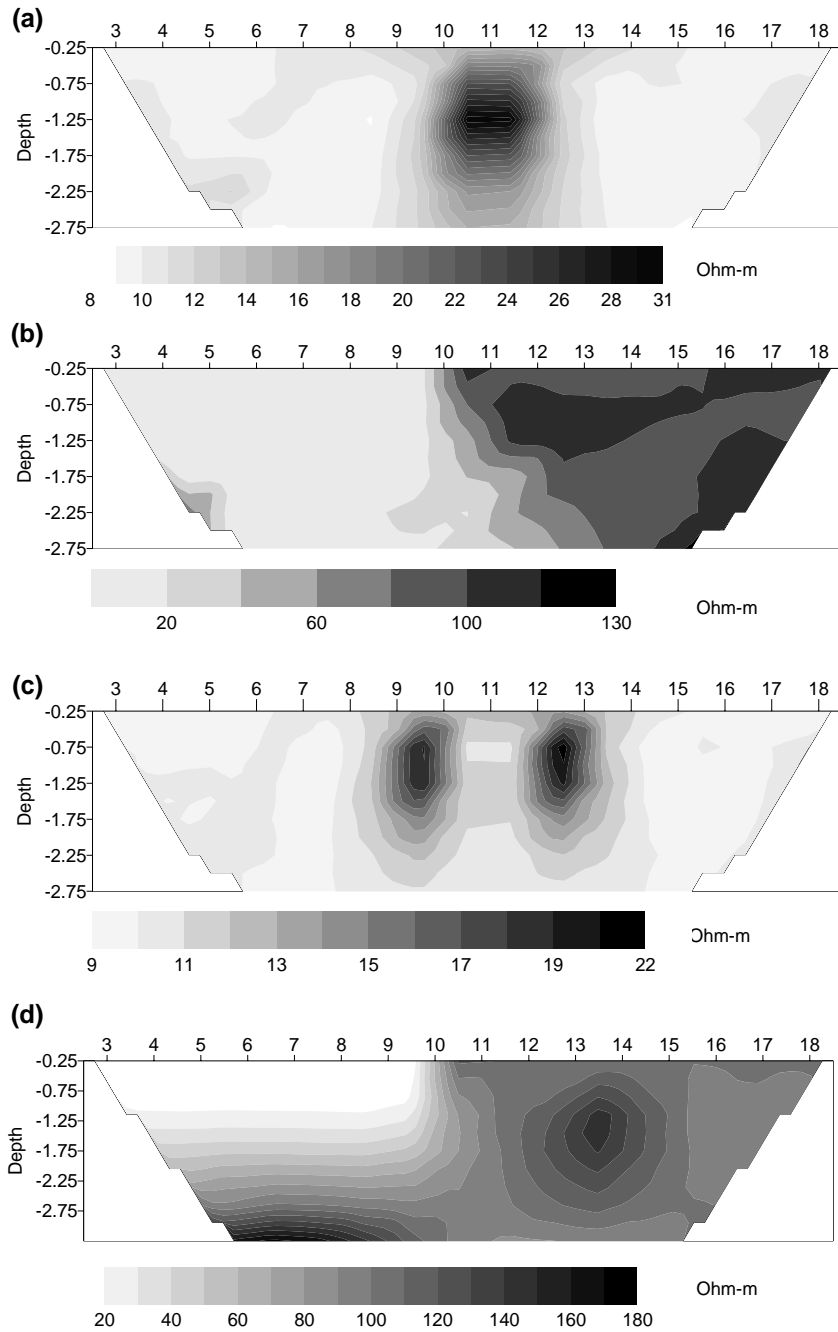
FIG. 7: Reconstruction of dipole-dipole data using the generalized BP scheme: a) Model 2 (9 iterations, 5.8% RMS error), b) Model 3 (6 iterations, 6.3% RMS error), c) Model 4 (11 iterations, 8.1% RMS error).

Real data reconstructions

The algorithm was tested with real data. The results presented here are from archaeological sites where the position and the characteristics of the targets are generally known. Therefore, the reconstructed images can be directly tested against the known targets and in this way an objective validation of the algorithm can be made.

Roman cemetery (Europos, N. Greece): The first case study is from the archaeological site of Europos (N.Greece). Based on a resistivity map from the area of the Roman cemetery of the ancient town (see Fig. 8), dipole-dipole data-sets, were collected. Two measured sections (AB, MN) (see Fig. 8) were taken over the centre of high resistivity features which are revealed on the map. These features have been interpreted as tombs (Tsokas et al., 1991) and this interpretation was later verified by the excavation results. The inter-electrode spacing was 1 m, the maximum n

separation was 8 and 16 electrodes were used (76 data - points).
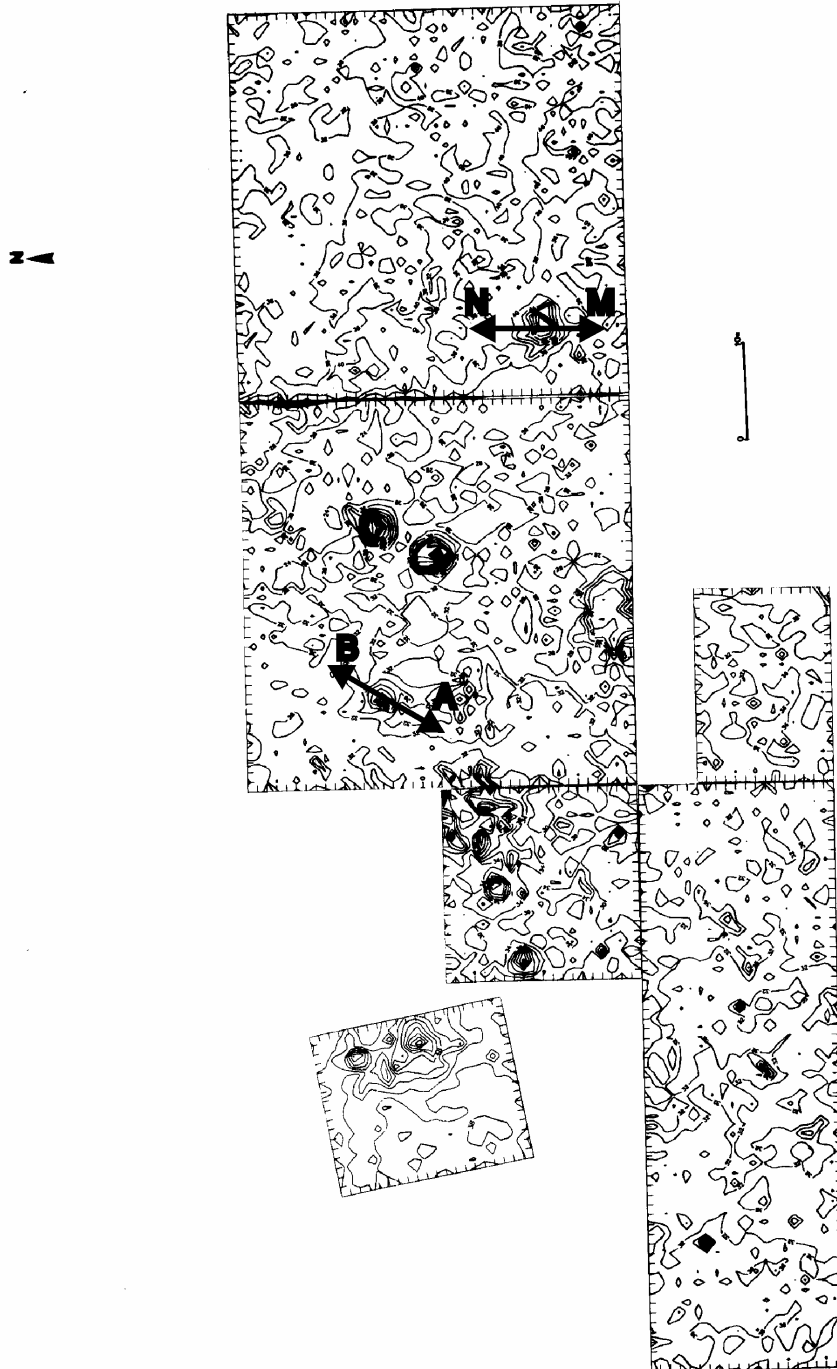
FIG. 8: Resistivity contour map obtained from the area of the ancient cemetery of Europos. The observed resistivity anomalies have been interpreted as tombs (Tsokas et al., 1991). The measured sections (AB), (MN) are shown as well.

The pseudosection of the data-set AB is depicted in Figure 9a and the generalized back-projection reconstruction after 9 iterations (RMS error 9.4%) can be seen in Figure 9b. The excavation revealed a rectangular grave: its approximate position and dimensions in relation to the measured section can be seen in Figure 9c. The BP reconstruction is in good agreement with the excavation results.

(a)

A →→→→→→→→→→→→→→→→→→→ B

Distance (m)

(b)

Distance (m)

(c)

Distance (m)
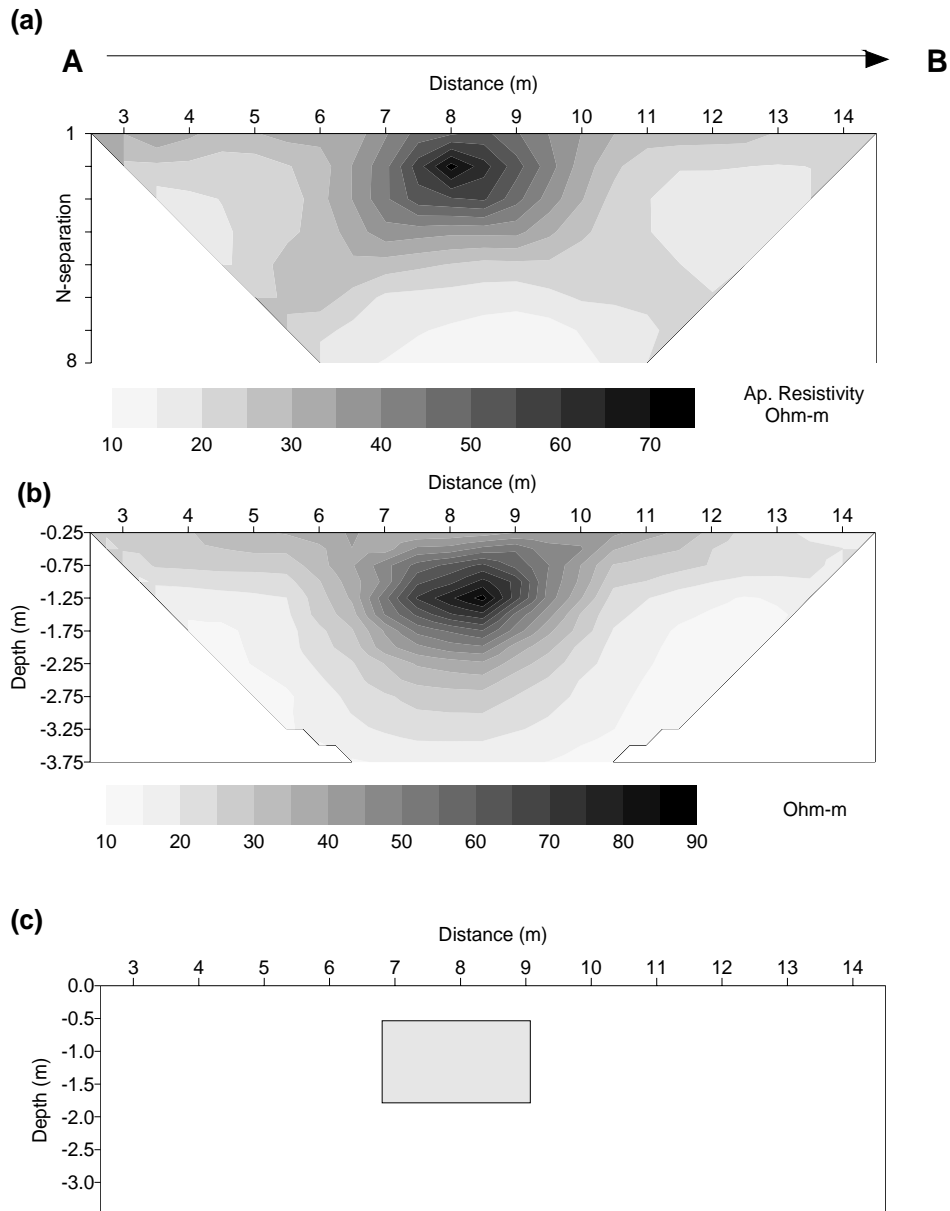
FIG. 9: Reconstruction of dipole-dipole data measured over a tomb at the roman cemetery of Europos (N. Greece) (section AB): a) the measured data-set in a pseudosection form, b) reconstruction using the generalized BP algorithm (9 iterations, 9.4% RMS error), a) the approximate location of the excavated tomb in relation to the measured section.

In Figure 10a the pseudosection of the data-set MN is shown. Note that the pseudosection image is quite complicated. The generalized back-projection reconstruction after 11 iterations (RMS error 12.2%) can be seen in Figure 10b. The excavation revealed a grave with a collapsed roof: its approximate position and dimensions in relation to the measured section can be seen in Figure 10c. The reconstruction produced useful information about the shape and the location of the anomaly (the side walls of the tomb can be distinguished), and they are in agreement with the excavation results. Fountains Abbey, (N. Yorkshire): Two case studies from the Fountains Abbey world heritage site are presented here. The fist case study is from the guest hall area. A detailed twin-probe profiling survey at the site revealed the foundations of the guest hall at the Western side of the Abbey (Szymanski et al., 1992).
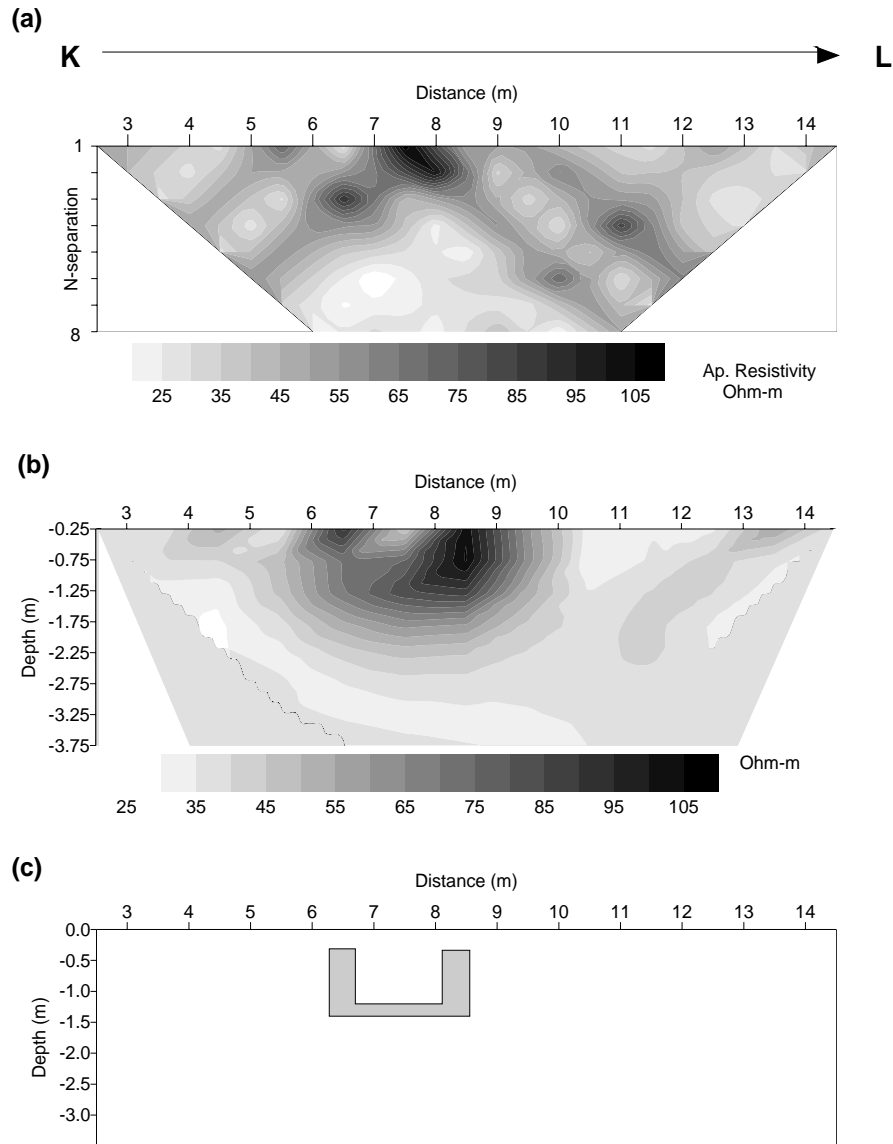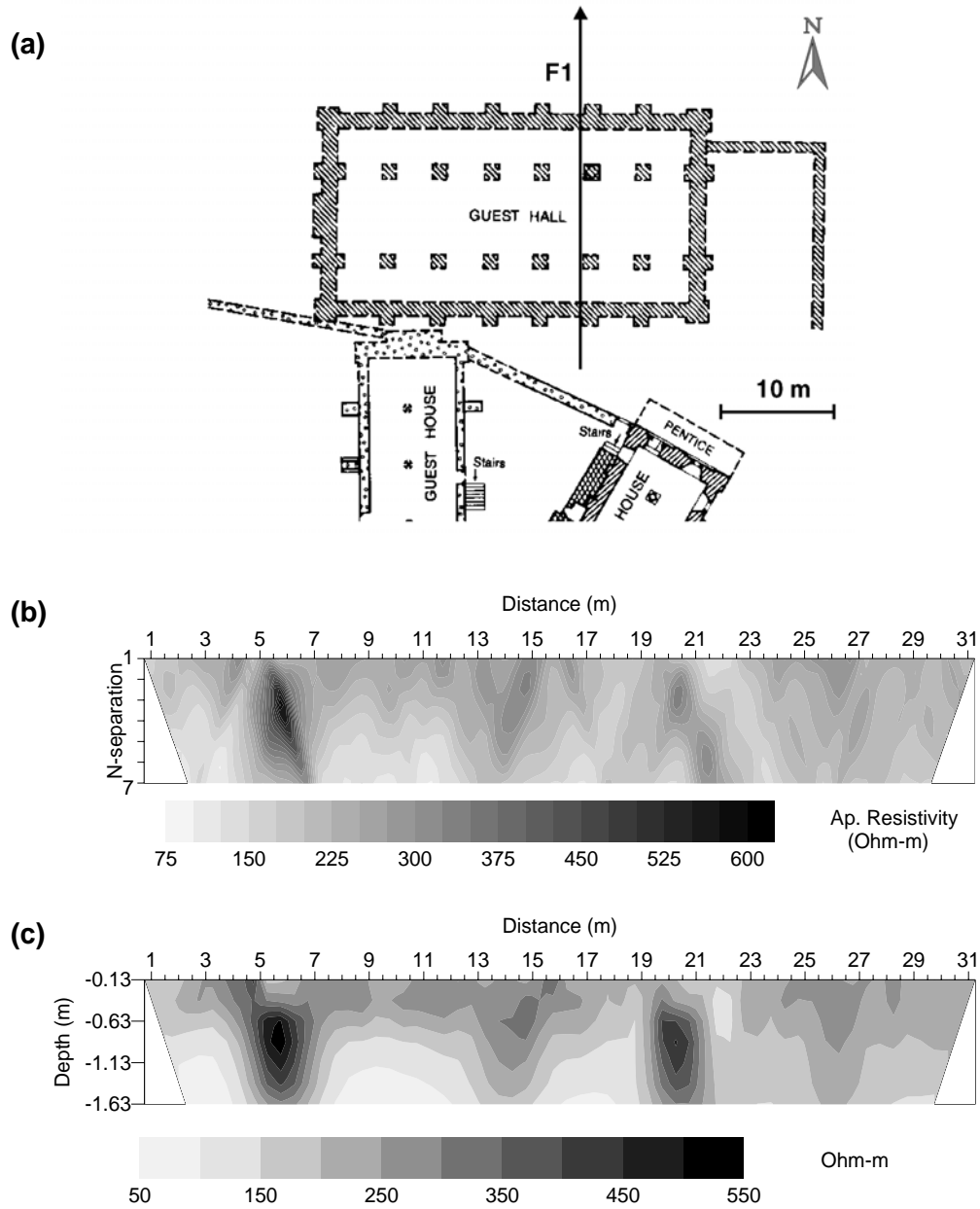
FIG. 10: Reconstruction of dipole-dipole data measured over a tomb at the roman cemetery of Europos (N. Greece) (section MN): a) the measured data-set in a pseudosection form, b) reconstruction using the generalized BP algorithm (11 iterations, 12.2% RMS error), a) the approximate location of the excavated tomb in relation to the measured section.

The plan of the guest-hall after the interpretation of the resistivity survey is depicted in Figure 11a.

A dipole-dipole data-set was obtained over the section F1 (the section is also depicted in Figure 11a) with a South-to-North direction. A total of 65 electrodes positioned 0.5 m apart were used and the maximum n-separation was $n=7$ (413 measurements). The pseudosection results are shown in Figure 11b and the BP reconstruction (11 iterations, 7.5% RMS error) is shown in Figure 11c. The reconstructed image produced two major resistive features which coincide exactly with the location of the wall foundations. Further, a less resistive region situated at the middle of the section can be due to the side-effect of the pillar foundations which are located quite close to the measuring section (20 cm). The reconstruction positioned the upper limits of the walls at a depth of approximately 50 cm. This depth is probably unrealistic - the real depth should be around 20-30cm (Emerick, 1995 personal communication).

(a)

(b)

Distance (m)

Ap. Resistivity
(Ohm-m)

(c)

Distance (m)

Ohm-m

FIG. 11: Reconstruction of dipole-dipole data measured over the area of the Guest-Hall at Fountains Abbey (N. Yorkshire): a) the location of the section in relation to the Hall's foundations, b) the measured data-set in a pseudosection form, c) reconstruction using the generalized BP algorithm (11 iterations, 7.5% RMS error.

The second case study is from the area of the mill of the Abbey. A drain runs across a narrow strip of land which is enclosed by the river Skell. A dipole-dipole data-set (24 electrodes 1m apart, maximum n=7) was obtain over a section situated orthogonally to the drain. The edge of the drain is visible and its position in relation to the measured section is depicted in Figure 12a. The pseudosection of the data-set is depicted in Figure 12b - note that the pseudosection slightly misplaces the target to the left. The generalized back-projection reconstruction after 9 iterations (RMS error 6.3%) can be seen in Figure 12c. The BP results are in very good agreement with the reality - both the position and the size of the drain is successfully reconstructed.
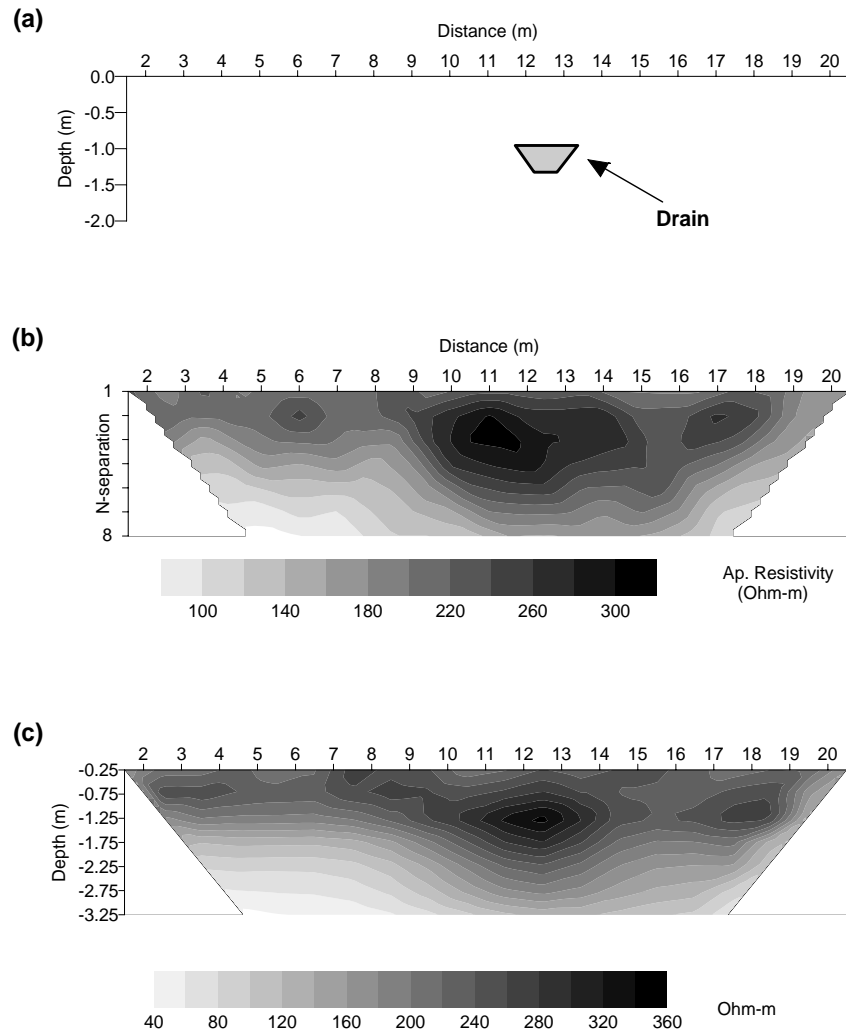
FIG. 12: Reconstruction of dipole-dipole data measured over a drain at the Fountains Abbey (N. Yorkshire): a) the exact location of the drain in relation to the measured section, b) the measured data-set in a pseudosection form, c) reconstruction using the generalized BP algorithm (9 iterations, 6.3% RMS error).

DISCUSSION AND CONCLUSIONS

The described algorithm although by no means theoretically correct, is physically reasonable. The back-projection procedure can be viewed as a pseudo-inverse operation: following Shima (1992) if J is the Jacobian matrix the back-projection approximates J^{-1} by WJ^T where W is a diagonal matrix whose elements are the inverse of the sum of the sensitivities related to each measurement.

Because of its approximate nature the convergence of the algorithm is not guaranteed, nor can the speed of the convergence be predicted. Divergence may sometimes occur when the data

noise is high. The convergence, if there is convergence at all, can be speeded up by the use of an over-relaxation factor within the reconstruction algorithm. In most of the tested cases the algorithm presented stable convergence behaviour and usually took less than 10 iterations to reach to a minimum error.

Barker (1992) referred to possible inherent problems with simple back-projection methods when near-surface lateral changes in resistivity occur (especially when arrays sensitive to such types of resistivity anomalies are used) and he suggested that these effects can be propagated and projected deeper creating artefacts. This can be true in the case of simple graphical back-projection schemes such as Bristow's method.

Though it should be borne in mind that full back-projection is a summation procedure so that the correction factor for each parameter is influenced by all the measurements that affect this parameter. Therefore, the effect of an individual measurement needs not to be decisive for determining any particular resistivity. Moreover, in the current scheme, the existence of the weighting terms are another factor which limit the propagation of the lateral effects with depth is limited. The results presented here verify this observation.

Despite its approximate nature the algorithm can give useful reconstructions of the subsurface resistivity and has proved to be stable and reliable in the cases tested. The tests with synthetic data indicated that the algorithm: (a) can produce reconstructions which do not suffer from major artefacts, (b) can produce reasonably accurate qualitative and quantitative reconstructions and (c) it is relatively noise-insensitive.

The tests with of real data indicated that the algorithm produced results that are generally in good agreement with the known targets. In some case-studies (of generally complicated nature) failed to delineate the depth of the targets successfully. These problems are due to its approximate nature. For the same reason the RMS errors were not particularly low.

Compared to existing schemes the main advantage of the proposed algorithm is that it is computationally fast compared to typical non-linear schemes since it avoids the matrix inversion procedure. Note that the matrix inversion procedure when very large data-sets (i.e. fully tomographic, 3D) are considered is extremely time consuming.

Overall, it is believed that the algorithm can serve as a practical tool for the preliminary interpretation of tomographic resistivity data. Moreover the reconstructed images can be used as initial estimates for accurate inversion schemes.

REFERENCES

Barber, D.C., Brown, B.H., and Freeston, I.L., 1983. Imaging spatial distributions of resistivity using applied potential tomography. Electronic Letters, 20: 933-935.

Barker, R., 1992. A simple algorithm for electrical imaging of the subsurface. First Break, 10: 53-63.

Bristow, C.M., 1966. A new graphical resistivity technique for detecting air-filled cavities. Study in Speleology, 1: 204-227.

Coggon, J.H., 1971. Electromagnetic and electrical modelling by the finite element method. Geophysics, 36: 132-155.

Dahlin, T. 1993. On the automation of 2D resistivity surveying for engineering and environmental applications. Ph.D. Thesis, Lund University.

Edwards, L.S., 1977. A Modified Pseudosection for Resistivity and IP. Geophysics, 42: 1020-1036.

Griffiths D., Turnbull, J., and Olayinka, A., 1990. Two-dimensional resistivity mapping with a computer-controlled Array. First Break, 8: 121-129.

Noel, M., and Walker R., 1991. Imaging archaeology by electrical resistivity tomography: a preliminary study. in Archaeological sciences 89, Budd, P., Chapman, B., Jackson, C. Janaway, R. and Ottaway, B., Oxbow, 295-304.

Noel, M., 1992. Multielectrode resistivity tomography for imaging archaeology: in Geoprospection in the Archaeological Landscape, Spoerry, P. (ed.), Oxbow Monograph 18: 89-99.

Pelton, W., Rijo, L., and Swift, J., 1978. Inversion of two-dimensional resistivity and induced polarization Data. Geophysics, 43: 788-803.

Powell, H.M., Barber, D.C., and Freeston, I.L., 1987. Impedance imaging using linear electrode arrays. Clin. Phys. Physiol. Meas. Suppl.A, 8:109-118.

Rijo, L., 1977. Modelling of electric and electromagnetic data. Ph.D. Thesis, University of Utah.

Smith, N., and Vozoff, K., 1984. Two-dimensional DC resistivity inversion for dipole-dipole data. IEEE Trans. Geosc., 22: 21-28.

Shima, H. and Sakayama, T., 1987. Resistivity tomography: An approach to 2-D resistivity inverse problems. 57th SEG meeting, Expanded abstracts, 204-207.

Shima, H., 1992. 2-D and 3-D resistivity image reconstruction using crosshole data. Geophysics, 57: 1270-1281.

Stretenovic, B., and Marcetic, D., 1992. Determination of the internal geometry of a land-slide using electrical tomography. Abstracts of the 54th Meeting of the E.A.E.G., Paris, France, 1-5 June.

Szymanski J., Cambell T., Dittmer J, Giannopoulos A., Tsourlos P., Coppack P., Emerick K. and Wilson K. (1992). Non-destructive site diagnosis at medieval abbey sites in the UK. Proceeding of MEDIEVAL EUROPE 1992, York, U.K., 21-24 September 1992, 201-206.

Telford, W., Geldart, L., Sheriff, R., and Keys, D., 1991. Applied geophysics. Cambridge University Press.

Tripp, A., Hohmann, G., and Swift, C., 1984. Two-dimensional resistivity inversion. Geophysics, 49:1708-1717.

Tsokas G., Giannopoulos A., Tsourlos P., Vargemezis J., Tealby J., Sarris A., Papazachos C., and Savopoulou T., 1994. A large scale geophysical survey in the archaeological site of Europos (N.Greece). Journal of Applied Geophysics, 32:85-98.

Tsourlos P., 1995. Modelling interpretation and inversion of multielectrode resistivity survey data. Ph.D. Thesis, University of York.

Yorkey, T., Webster, J., and Tompkins, W. 1987. Comparing reconstruction methods for electrical impedance tomography. IEEE Trans. Biom. Eng., 34: 843-852.